Flow Mechanism of Cooling Effectiveness Improvement for the Cylindrical Film Cooling Hole with Contoured Craters

Flow Mechanism of Cooling Effectiveness Improvement for the Cylindrical Film Cooling Hole with Contoured Craters

Linchao Bai[1, 2], Chao Zhang[1, 2]

[1]Tianjin Key Laboratory for Advanced Mechatronic System Design and Intelligent Control, 300384 Tianjin, China
[2]National Demonstration Center for Experimental Mechanical and Electrical Engineering Education (Tianjin University of Technology), Tianjin 300384, China

Abstract. In this paper, a typical cylindrical hole with contoured craters is investigated in terms of the downstream flow field by numerical method at blowing ratios of 0.5, 1 and 1.5. The flow field and the cooling effectiveness are analyzed using three-dimensional Reynolds-averaged Navier-Stokes equations with the shear stress transport turbulence model. In comparison to the cylindrical hole, the cratered hole shows a wider coolant coverage in lateral direction and a lower penetration into the mainstream flow due to the larger hole exit area. Moreover, the interaction between the coolant and the curved protrusion induces a new anti-kidney-shaped vortex pair, which can obviously improve the cooling coverage and thus the cooling effectiveness. The area-averaged cooling effectiveness for the cratered hole is always higher than that for the cylindrical hole at all three blowing ratios.

1. Introduction

Film cooling and thermal barrier coating (TBC) are widely used simultaneously to reduce the thermal load of gas turbine vanes/blades in order to enable higher turbine inlet temperature. Hence, new efficient but simple configurations based on the cylindrical hole may occur if the TBCs are sprayed with a special designed manner. Two kinds of typical novel configurations are the shallow trench slot [1] and the crater [2]. The geometrical difference is caused by a continuous slot-like mask around a row of holes for the trench slot but discrete masks around every discrete hole for the crater. In spite of higher cooling effectiveness for the trenched hole, the cratered hole may be a better choice especially in consideration of the thermal stress [3]. Another disadvantage of trenched hole is that the regions between cooling holes may be warmed by the invading hot gases [4]. Thus present study is mainly focused on the cratered hole.

Relevant studies [2, 5] showed that the adiabatic cooling effectiveness can improve by adopting a proper crater shape. The circular cratered hole performs better than the concentric elliptical cratered hole and the upstream offset ellipse cratered hole. Zhang et al [6] numerically evaluated five different cratered holes at a lower blowing ratio of 0.5, but found the concentric elliptical cratered hole performs best. Kim et al [7] carried out a design optimization of cratered cylindrical hole at blowing ratio of 0.5, and found an elliptical shape with wider lateral coverage showing the maximum area-averaged adiabatic cooling effectiveness. Khalatov et al [8] proposed two types of new cratered holes with hemispherical and triangular shape. Through their numerical analysis of a flat plate film cooling, the triangular shape showed better coolant lateral spreading, and thus improved adiabatic cooling effectiveness at blowing ratios higher than 1.0. Kalghatgi and Acharya [9] proposed a cratered hole with contoured shape and evaluated numerically at blowing ratios of 1.0 to 2.5. The key feature of this novel design was a blunt V-shaped protrusion toward the downstream end of cylindrical hole. An et al

[10] proposed a so-called near surface streamwise diffusion hole and investigated the adiabatic cooling effectiveness experimentally. The most improvement of this design was increasing the exit area with both lateral and streamwise expansions as the traditional shaped hole, which could lower the coolant momentum flux.

Recently, the double wall cooling concept [11] with thinner blade thickness has was proposed, which results in film cooling holes with short hole length-to-diameter ratio. Lutum and Johnson [12] analyzed the influence of hole length-to-diameter ratio of cylindrical hole ranged from 1.75 to 18 on adiabatic cooling effectiveness. They pointed out that due to the undeveloped flow in the hole and larger effective injection angle with respect to the wall, the adiabatic cooling effectiveness generally decreases with decreasing hole length-to-diameter ratio in the range of 1.75 to 5. Thus, the cratered hole with hole length-to-diameter ratio of 6 proposed in [10] is needed to be reassessed in condition of short hole length-to-diameter ratio.

Based on the novel cratered configuration proposed in [10], the present paper aims to investigate the flow mechanism of cooling effectiveness compared with the cylindrical hole. The adiabatic cooling performance at blowing ratios ranged from 0.5 to 1.5 will be also compared.

2. Physical model and numerical setup

2.1. Physical model

The physical model consists of a mainstream passage, a cratered cylindrical hole and a coolant plenum, which is shown in figure 1. The cylindrical hole has a diameter D=12.7mm, and the hole length-to-diameter is 3. The geometry of each component is also depicted in figure 1. The hole pitch has a typical value of 3D. The coordinates X, Y and Z denote the streamwise, lateral and vertical directions respectively.

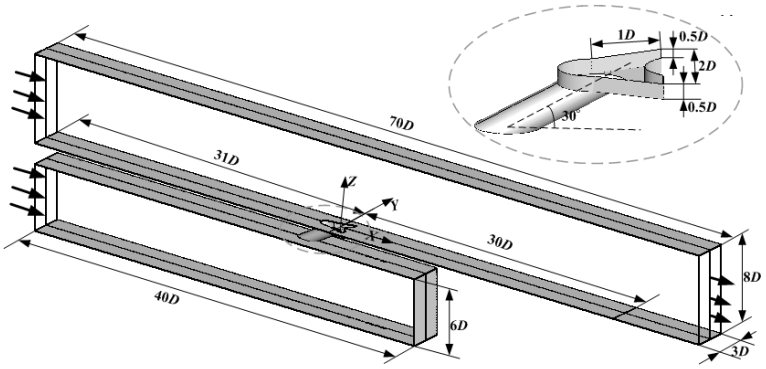

Figure 1..The physical model.

2.2. Numerical method and boundary conditions

Three dimensional RANS analysis of flow fluid and heat transfer are performed by software ANSYS CFX. This software solves the Reynolds-averaged Navier-Stokes equations (RANS) and uses the k-ω based shear-stress transport (SST) two-equation turbulence model to compute the averaged turbulent stresses. The k-ω SST turbulence model was validated for the film cooling simulations in the previous numerical works [13, 14]. Thus, in present simulations, the k-ω SST turbulence model is selected. The advection and turbulence terms are both solved with high resolution schemes. When the root mean square residuals of all variables are less than 10^{-6}, the simulations are regarded to achieve convergence.

The geometry of computational domain is created by using the software ICEM CFD. Due to the symmetric geometry by the plane Y/D=0, half of the physical model ($0 \le Y/D \le 1.5$) is adopted to save computational cost. The planes Y/D =0 and 1.5 are set as symmetric boundaries, and all other walls are treated as adiabatic no-slip conditions. The inlet boundary for the mainstream passage is a uniform velocity of 12.8m/s at a temperature of T_m=321K. The inlet temperature of coolant plenum is set as T_c=296K to obtain the coolant-to-mainstream density ratio of 1.08, which equals to the value in [5].

Also the inlet boundaries are set as uniform velocities of 0.2776m/s, 0.5552m/s and 0.8328m/s for the given blowing ratios M =0.5. 1.0, and 1.5 respectively. The outlet condition of mainstream passage is a constant static pressure of 0.1MPa.

The structured meshes are also generated by the software ICEM CFD. The grids are refined around all the walls including the hole and crater. The first grid point away from the wall is placed to satisfy the values of y^+ around 1. The detailed meshes around the hole are shown in figure 2. After the grid independence checking, the total number of meshes is 1.735 million.

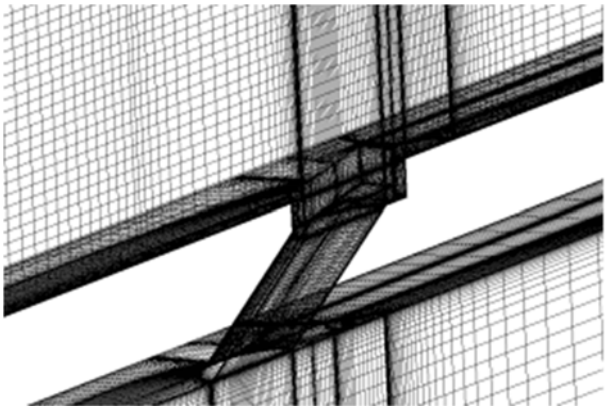

Figure 2. Computational meshes around the hole.

2.3. Data reduction

Among the many results of air film cooling, the cooling effectiveness is used to evaluate the cooling effect. The adiabatic cooling effectiveness can be calculated as

$$\eta = (T_m - T_c)/(T_{\mathrm{aw}} - T_c) \tag{1}$$

Where, T_{aw} is the adiabatic temperature over the flat-plate wall (K).

As an important indicator to evaluate the cooling effect of the film, the higher the value of η, the smaller the temperature difference between the flat-plate wall and the inlet temperature of coolant plenum, and the better the cooling effectiveness.

Because the cooling effectiveness can't reflect the film cooling effect quantitatively, the area-averaged cooling effectiveness $\overline{\eta}$ and the intensity of the vorticity in X direction ω_{X} are introduced.

The area-averaged cooling effectiveness is calculated over the interested downstream region ($0 \le Y/D \le 1.5$, $0 \le X/D \le 30$), which is given by

$$\overline{\eta} = \frac{1}{1.5D \times 30D} \int_0^{30D} \int_0^{1.5D} \eta \, dY dX \tag{2}$$

The intensity of the vorticity in X direction ω_{X} is used to illustrate the strength of vortex pair, which can be calculated as

$$\omega_{\mathrm{X}} = \partial U_{\mathrm{Z}}/\partial Y - \partial U_{\mathrm{Y}}/\partial Z \tag{3}$$

where U_{Z}, U_{Y} are the velocities in Z direction and Y direction, respectively.

In the following paragraphs, the vorticity distribution and the contour distribution cloud map of the streamline on the plane are generated to analyse the film cooling effect.

3. Results and discussion

3.1. Flow field

In order to better illustrate the flow mechanism of the cratered hole, a simple cylindrical hole is used for comparison. Figure 3 and 4 show the contours of velocity distribution in the Y and Z directions at the outlets of the hole and the crater with blowing ratio of 1 respectively. Note that the Y direction

velocity determines the lateral expansion capability of the coolant, and the *Z* direction velocity represents the penetration ability into the mainstream flow. It is obviously seen in figure 3 that the coolant is contracted towards to the hole center by the depression of the mainstream flow for the cylindrical hole. But for the cratered hole, the upper half part of the outlet appears a positive high *Y* direction velocity region and the lower half part occurs a negative high *Y* direction velocity region. These two regions promote the coolant with a wider lateral expansion, which is benefit for the coolant coverage. There is a large difference for the *Z* direction velocity distributions, which can be clearly seen in figure 4. Due to the bending effect along the cylindrical hole, a high *Z* direction velocity region occurs at the windward side of the hole outlet, a highest *Z* direction velocity region with slim shape locates nearby the hole centerline. Moreover, the whole outlet exhibits positive *Z* direction velocity at every location. For the cratered hole outlet, the average *Z* direction velocity decreases due to a higher area. A higher *Z* direction velocity region locates at the leeward side due to the blocking effect by the curved protrusion. A negative *Z* direction velocity region appears just downstream the windward side by the mainstream flow ingestion, which is a disadvantage for cooling effectiveness improvement. The mainstream flow ingestion will heat the coolant, and thus reduce the cooling capability.

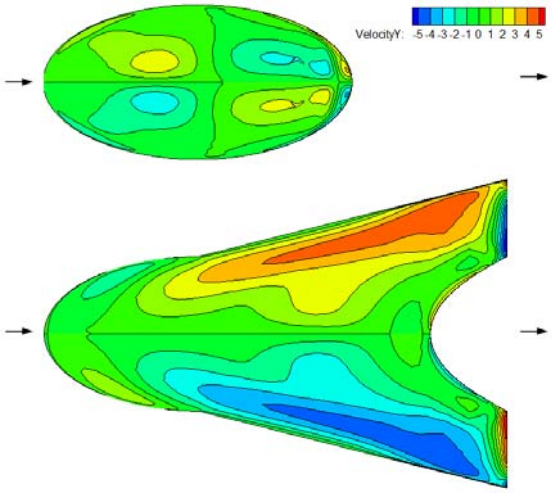

Figure 3. The contours of *Y* direction distribution at the hole outlets.

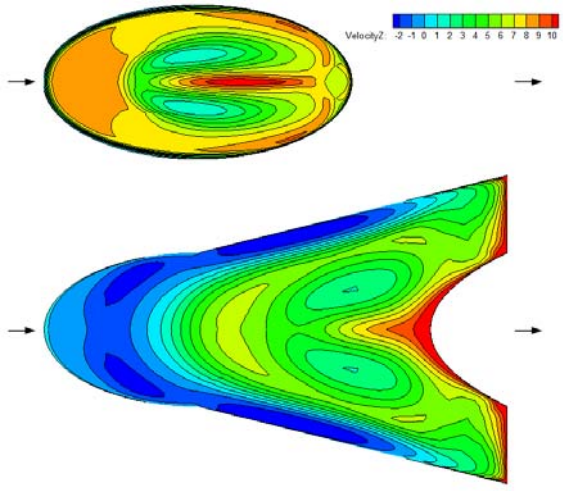

Figure 4. The contours of *Z* direction distribution at the hole outlets.

Figure 5 and 6 show the footprints of the vorticity ω_X and the streamlines over three planes *X*/*D*=0, 3.33 and 6.67 for the cylindrical hole and the cratered hole with blowing ratio of 1 respectively. It can

be seen from figure 5 that a kidney-shaped vortex pair is generated by the mutual influence between the mainstream flow and the coolant injection. The coolant injection is lift away from the wall in the vertical direction, and thus cooling performance is poor. Besides, a much smaller and opposite vortex pair is located just below the kidney-shaped vortex pair at plane X/D=3.33 and 6.67, which means the coolant is reattached to the wall. For the cratered hole in figure 6, the contour of vorticity distribution is similar as the cylindrical hole, except for a small opposite vortex pair at the outside in the lateral direction of the diffusion edges. At plane X/D=3.33, an anti-kidney-shaped vortex pair is generated by the curved protrusion, and breaks the original kidney-shaped vortex pair into two segments. This anti-kidney-shaped vortex pair can drag the coolant to flow away from the hole centerline, which is benefit for a wider coolant coverage. But the intensity of the anti-kidney-shaped vortex pair is not high enough to overcome the entrainment effect by the mainstream flow, thus is disappeared at plane X/D=6.67. So the coolant coverage in the lateral direction is degraded for the far downstream region from the hole exit.

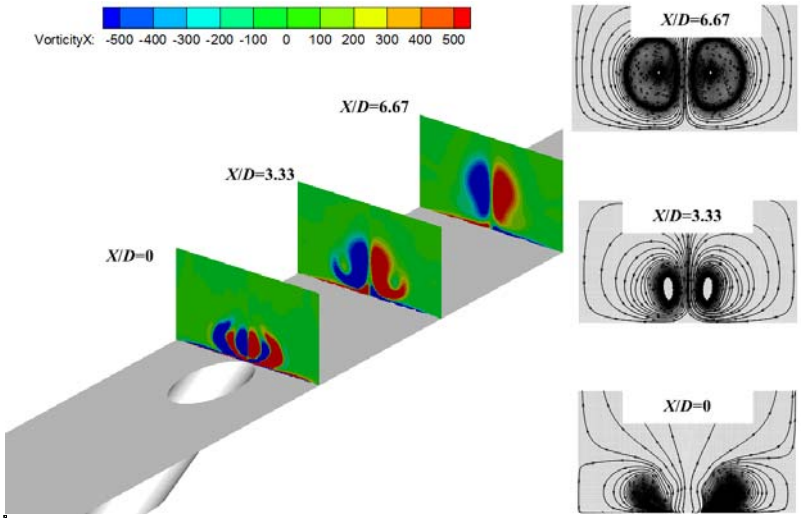

Figure 5. The contours of vorticity distribution and streamlines on planes X/D=0, 3.33 and 6.67 for the cylindrical hole.

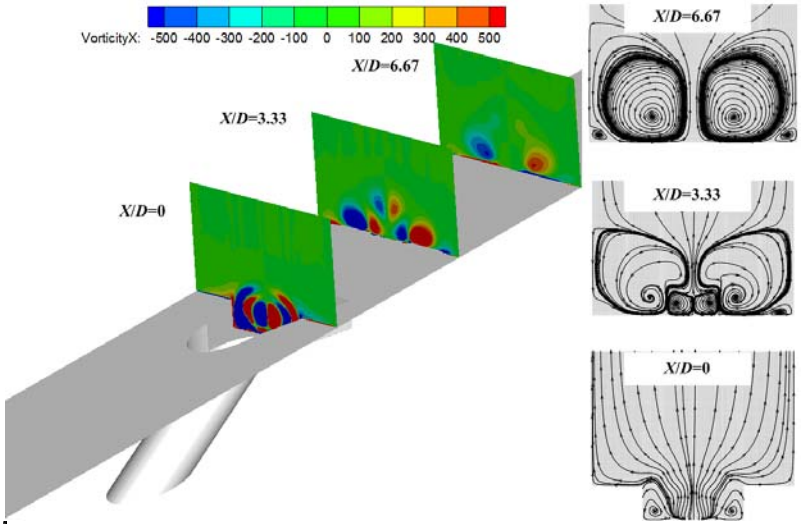

Figure 6. The contours of vorticity distribution and streamlines on planes X/D=0, 3.33 and 6.67 for the cratered hole.

3.2. Cooling effectiveness

The adiabatic cooling effectiveness distributions over the wall for the cratered hole and the cylindrical hole at three blowing ratios *M*= 0.5, 1 and 1.5 are shown in figure 7. It can see that the effective coolant coverage is much improved at any blowing ratio. A region of high cooling effectiveness is immediately observed just downstream the curved protrusion. At higher blowing ratios, the region high cooling effectiveness is still maintained, but the coolant flow towards away the centerline is much reduced. The reason is that the coolant penetration is higher into the mainstream flow, and less coolant is blocked by the curved protrusion, and thus the anti-kidney-shaped vortex pair with smaller intensity is generated.

In order to quantify the superiority of the cratered hole to the cylindrical hole, the area-averaged cooling effectiveness of both holes is given in table 1. Obviously, the cratered hole has positive influence on cooling effectiveness improvement at all three blowing ratios. The highest area-averaged cooling effectiveness with the value of 0.3025 is obtained at the lowest blowing ratio *M*=0.5. The area-averaged cooling effectiveness of cratered hole has a decreasing trend with the increasing of blowing ratio, which is consistent with the change trend of the cylindrical hole.

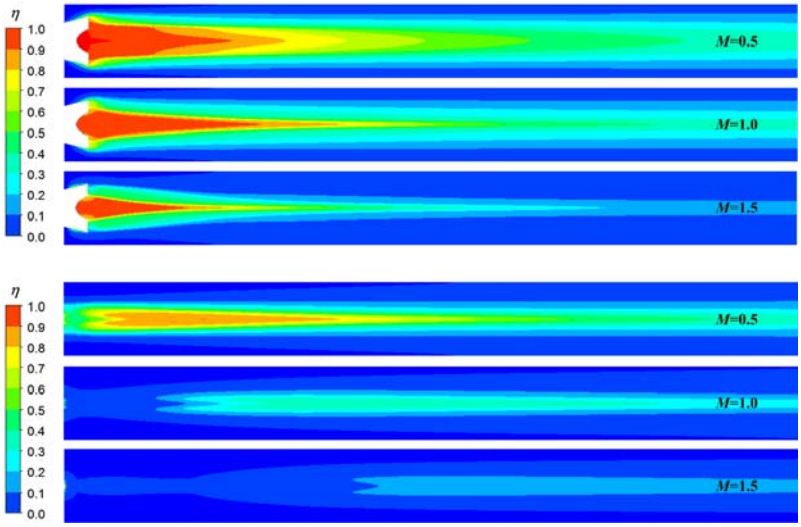

Figure 7. The cooling the effectiveness contours for the cratered hole and the cylindrical hole at three blowing ratios M= 0.5, 1 and 1.5.

Table 1. Area-averaged cooling effectiveness at different blowing ratios.

	M=0.5	*M*=1.0	*M*=1.5
Cylindrical hole	0.1837	0.0796	0.0357
Cratered hole	0.3205	0.2373	0.1177

4. Conclusion

The flow structure and cooling effectiveness are numerically investigated for both the cylindrical hole and the cratered hole at blowing ratio of 0.5, 1.0 and 1.5. The following conclusions can be drawn from the results of the presented work:

(1) In comparison to the cylindrical hole, the larger exit area for the cratered hole significantly alter the velocities distributions in *Y* direction and *Z* direction. This will help to improve the coolant coverage in the lateral direction and decrease the penetration height into the mainstream flow.

(2) The curved protrusion plays a key role on the generation of a new anti-kidney-shaped vortex pair. This will promote the increasing of coolant coverage in the lateral direction, and improve the cooling effectiveness significantly.

(3) The cratered hole always shows higher area-averaged cooling effectiveness than the cylindrical hole at blowing ratios of 0.5, 1 and 1.5. The area-averaged cooling effectiveness decreases with the increasing of blowing ratio.

Acknowledgments
The authors would like to acknowledge the financial support by the National Science Foundation of China (Grant No. 51506150) and the Natural Science Foundation of Tianjin (Grant No. 18JCQNJC07200).

References
[1] Bunker R S 2002 Film cooling effectiveness due to discrete holes with a transverse surface slot *Proc. ASME Turbo Expo 2002* GT2002-30178.
[2] Dorrington J R, Bogard D G, Bunker R S 2007 Film effectiveness performance for coolant holes imbedded in various shallow trench and crater depressions *Proc. ASME Turbo Expo 2007* GT2007-27992.
[3] Lee H L, Kim K M, Shin S, and Cho H H 2009 *J. Thermophys. Heat Transfer* **23(4)** 843-6.
[4] Davidson F T, Dees J E, and Bogard D G 2011 An experimental study of thermal barrier coatings and film cooling on an internally cooled simulated turbine vane, *Proc. ASME Turbo Expo 2011* GT2011-46604.
[5] Lu Y P, Dhungel A, Ekkad S V, and Bunker R S 2009 *J. Turbomachinery* **131(1)** 011005.
[6] Zhang Z W, Qian W J, and Hu J M 2016 *Key Eng. Mater.* **693** 491-7.
[7] Kim J H, and Kim K Y 2016 *J. Therm. Sci. Technol.* **11(2)** JTST0025.
[8] Khalatov A A, Panchenko N A, Severin S D 2017 *J. Phys.: Conf. Seri.* **891** 012145.
[9] Kalghatgi P, and Acharya S 2015 *J. Turbomachinery* **137(10)** 101006.
[10] An B T, Liu J J, Zhang X D, Zhou S J, and Zhang C 2016 *Int. J. Heat Mass Transf.* **103** 1-13.
[11] Ligrani P, Ren Z, Liberatore F, Patel R, Srinivasan R, and Ho Y H 2017 *J. Eng. Gas Turb. Power* **140(5)** 051901.
[12] Lutum E, and Johnson B V 1999 *J. Turbomachinery* **121(2)** 209-16.
[13] Zhang C, Liu J J, Wang Z, and An B T 2013 The effects of Biot number on the conjugate film cooling effectiveness under different blowing ratios *Proc. ASME Turbo Expo 2013* GT2013-94041.
[14] Wang Z, Zhang C, Chen Y, Du W J, and Xin G M 2017 *J. Propul. Technol.* **38(9)** 2038-45.